

Time-domain coherent anti-Stokes Raman spectroscopy for hydrogen gas in the Dicke narrowing region

Yu. S. D'yakov, S. A. Krikunov, S. A. Magnitskii, S. Yu. Nikitin, and V. G. Tunkin

Moscow State University

(Submitted 3 December 1982)

Zh. Eksp. Teor. Fiz. **84**, 2013–2025 (June 1983)

An experiment on time-domain coherent anti-Stokes Raman spectroscopy (time-domain CARS) of molecular hydrogen was performed in the pressure range 10^{-2} –10 atm. The experimental setup had a dynamic measurement range 10^5 and could reliably record the signal in the gas-pressure range to 10^{-2} Torr. A theory of time-domain CARS is developed for an inhomogeneously broadened transition with allowance for two mechanisms that dephase the molecular vibrations, viz. collisions and the Doppler effect. The waveform of the pulsed response of a gaseous medium to an external field is calculated at arbitrary pressures. It is shown that under definite conditions the time-domain CARS technique can be used to determine the real and imaginary components of the nonlinear susceptibility of the medium, $\chi^{(3)}(\omega)$, in contrast to the frequency-domain CARS, in which $|\chi^{(3)}(\omega)|^2$ is measured. The results of the theory agree with the obtained experimental data.

PACS numbers: 33.20.Fb, 33.70.Jg, 51.70.+f

INTRODUCTION

One of the principal problems of molecular spectroscopy is the determination and detailed analysis of the mechanism whereby molecular vibrations are dephased. Most interesting in this respect are monatomic molecules, as well as molecules in excited vibrational states, for which the mechanism of the relaxation due to intermode intramolecular interaction has been little investigated so far. For simpler systems, however, particularly for diatomic molecules, there are a number of unsolved problems concerning the time evolution of the state of a coherently excited molecule ensemble.

Both frequency-domain and time-domain spectroscopy variants were used to investigate dephasing in molecular gases. In particular, dephasing of Raman-active vibrations of molecules was investigated by the methods of spontaneous spectroscopy,^{1,2} stationary active spectroscopy with pulsed³ and continuous pumping,^{4,5} and by the method of SRS amplification.⁶ The dephasing of IR-active vibrations was investigated by infrared absorption spectroscopy.⁷ Pulse methods were used to investigate one-photon IR-active vibrational and rotational transitions in molecular gases.^{8–11} The investigations revealed coherent nonstationary effects such as damping of the free polarization, optical nutation, or photon echo, while the characteristic relaxation times were in the microsecond range.

New means of investigating dephasing processes are uncovered by the method of stationary (time-domain) active spectroscopy, which permits direct observation of vibration dephasing in an ensemble of atoms or molecules.^{12–19} The physical information is extracted in this case from the shape of the pulsed response, which may turn out to be more amenable to measurements than the line shape and width in spectral methods. This applies in particular to narrow Raman resonances in molecular gases.

We use in this study the method of time-domain (nonstationary) coherent spectroscopy (time-domain CARS) to

investigate the simplest system—molecular hydrogen. The shape of the pulsed response is measured in detail at pressures from 5 Torr to 10 atm. The theoretical analysis is aimed at a quantitative interpretation of the experimental data. To this end it is necessary to calculate the shape and duration of the pulsed response measured in the time-domain CARS in the entire gas-pressure range, from the Doppler limit to the homogeneous broadening region, including the Dicke-narrowing region.

EXPERIMENTAL TECHNIQUE

The molecular vibrations are excited in CARS by biharmonic pumping at frequencies ω_1 and ω_2 , whose difference is close to the frequency of the investigated Raman resonance: $\omega_1 - \omega_2 \approx \omega_0$. The quantum and time diagrams of the excitation and sounding of the line $Q_{01}(1)(\nu_0 = 4155 \text{ cm}^{-1})$ of molecular hydrogen by the time-domain CARS method are shown in Fig. 1. The vibrations are excited by an amplified single picosecond pulse separated from a train of pulses from a neodymium-garnet laser operating in the passive mode-locking regime. The excitation wavelength is $\lambda = 1.06 \mu\text{m}$ and the duration of a single pulse is 40 psec. The second exciting pulse is produced by a picosecond parametric light

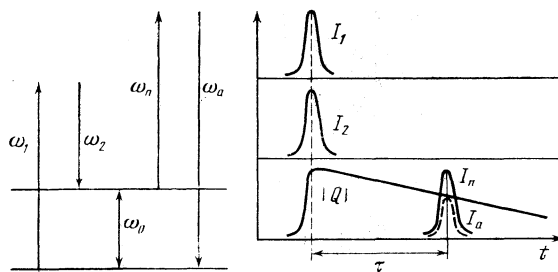


FIG. 1. Quantum and time diagrams of time-domain active Raman spectroscopy (CARS).

generator (PLG) with wavelength tunable in the range $\lambda_2 = 1.3 - 4.5 \mu\text{m}$, with two LiNbO_3 crystals (pump wavelength $1.06 \mu\text{m}$, pulse duration 40 psec). The width of the PLG emission spectrum was approximately 100 cm^{-1} . The vibrations were probed by recording a second-harmonic pulse of a neodymium laser ($\lambda_p = 0.53 \mu\text{m}$) scattered into the anti-Stokes region. The pulse of this laser could be made to lag the exciting pulses by a variable delay line. All the light waves had identical linear polarization. The radiation entering the gas-filled cell was focused onto its center by a lens of focal length 155 mm. The energies of the exciting and sounding pulses were respectively $W_1 = 5$, $W_2 = 0.3$, and $W_p = 3 \text{ mJ}$. This made possible reliable registration of the anti-Stokes scattering signal in the hydrogen pressure range down to 10^{-2} Torr . At a hydrogen pressure 10 Torr and zero delay of the probing pulse, the anti-Stokes pulse contained 10^8 photons. The delay range was $0 \leq \tau \leq 1.2 \text{ nsec}$ and ensured observation of the anti-Stokes pulse in its entire damping range. The use of pulses of approximate duration 40 psec guarantees that the pulsed-response shape are independent of the parameters of the exciting and sounding pulses.

The energy p_f the anti-Stokes pulse was subject to considerable fluctuations, mainly because of the instability of the spectrum of the picosecond PLG. When measuring the pulsed response, i.e., the dependence of the anti-Stokes radiation energy on the probing pulse delay, we used an average of 100 pulses. A more detailed description of the experimental procedure is given in Refs. 17 and 18.

In the employed range of hydrogen pressures and probing pulse delay times, the anti-Stokes radiation energy changed by approximately 5–6 decades. This, as well as the fact that the signal fluctuated considerably, made it desirable to expand the dynamic range of the recording system. To this end, the signal from the FÉU-39 photomultiplier used to register the anti-Stokes radiation energy was fed to two amplifiers, with gains 97 and 1, respectively. Each amplifier was connected to its own analog-digital converter (ADC), from which the information was fed through a matching device into a minicomputer. The latter was programmed for further calculations, depending on the magnitude of the signal, and of the output of either of the ADC, with allowance for the gains of the amplifiers preceding the ADC. A schematic block diagram of the setup is shown in Fig. 2.

The signal-energy measurement channel was calibrated using a set of calibrated neutral light filters. The small non-linearity due at maximum signals to the photomultiplier saturation at large currents was eliminated by the computer

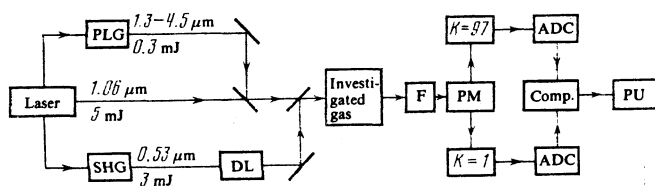


FIG. 2. Block diagram of experimental setup. System elements: SHG—second-harmonic generator, DL—delay line, F—filter, PU—printer unit. The remaining symbols are explained in the text.

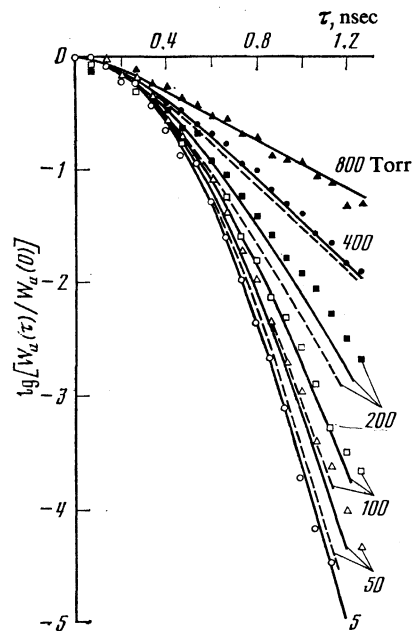


FIG. 3. Time-domain CARS of hydrogen. The points show the experimental data, the continuous curves are plots of Eqs. (16) and (21)–(23), dashed—Eqs. (17) and (21)–(23). The gas pressure ranges from 5 to 800 Torr.

program. The dynamic range of the signal measurement channel spanned thus approximately five decades. In a number of cases, however, this dynamic range was insufficient to cover the entire signal range. In such cases the signal was recorded at two voltages on the photomultiplier, with allowance for the change in the photomultiplier gain.

EXPERIMENTAL RESULTS

We measured in the experiments the dependence of the energy of the anti-Stokes pulse $W_a(\tau)$ on the time τ that the probing pulse lagged the exciting pulses. This dependence is shown in logarithmic scale in Figs. 3 and 4. Each set of points corresponds to a definite hydrogen pressure, which was varied from 5 Torr to 10 atm.

The results show that when the hydrogen pressure is increased the contour of the response pulse changes from Gaussian to exponential. The dephasing time τ_{ph} , defined as the time required for the response pulse to fall to a certain level, first increases with increasing pressure, and then decreases. The dephasing time has a maximum at a pressure 3 atm.

A more detailed examination makes it possible to distinguish on the experimental curves three characteristic sec-

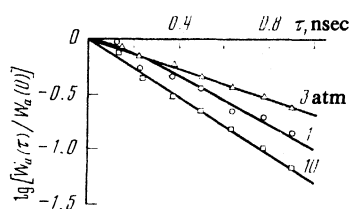


FIG. 4. The same as Fig. 3, pressure from 1 to 10 atm.

tions: quadratic, where $\log W_a(\tau) \propto -\tau^2$ (region of small delays), linear where $\log W_a(\tau) \propto -\tau$ (region of large delays), and intermediate. When the pressure is increased the first of these sections becomes narrower and the second broader. The $\log W_a(\tau)$ curve obtained at 5 Torr contains only the quadratic section, and that obtained at pressures higher than 2 atm only a linear section.

THEORY OF TIME-DOMAIN ACTIVE SPECTROSCOPY FOR AN INHOMOGENEOUSLY BROADENED TRANSITION

For a qualitative and quantitative interpretation of the experimental data it is necessary to calculate the time-domain CARS signal of a solitary Raman resonance in a large range of pressures of the molecular gas, from the Doppler limit to the homogeneous-broadening region, including the Dicke-narrowing region.

The contour of the pulsed response in the limiting cases of high and low pressures was investigated earlier (see, e.g., Ref. 19). It is well known thus that in high-pressure gases (homogeneous broadening region)^{18,19} and in liquids^{12,13} the pulsed response is exponential. In low-pressure gases^{14,16,19} the pulsed response is Gaussian. As for the contour of the response pulse at arbitrary gas pressure, the question remains open to this day.

In our theoretical description of coherent Raman scattering of light in a gas we shall take into account two mechanisms of the dephasing of molecular vibrations, collisions and the Doppler effect. The problem was considered in this formulation in many papers devoted to the theory of spectral-line broadening in gases (see, e.g., Refs. 1, 3, 8, 9, 11, and 20–28). The collisions between the molecules are usually taken into account by introducing a collision integral into the kinetic equation for the distribution function.^{22,24–28,8,11} In another approach^{20,21,3} use is made of the results of the theory of Brownian motion.²⁹

In our opinion, the Doppler dephasing of molecular vibrations, with allowance for the change in the change of the molecule velocities by the collisions, is simplest to describe within the framework of the frequency-modulation model developed in statistical physics (see, e.g., Ref. 30, Chap. 2). The mathematical problem reduces then to an analysis of a known linear differential equation with a randomly varying coefficient.^{31–33}

To calculate the CARS signal we use the equations

$$\frac{\partial q_j}{\partial \theta} + \left[\frac{1}{T_c} - ik_0 v_j(\theta) \right] q_j = \gamma_a A(\theta), \quad A = A_1 A_2^*, \quad (1)$$

$$Q = \frac{1}{N} \sum_{j=1}^N q_j, \quad \frac{\partial A_a}{\partial z} = \gamma_a A_p Q. \quad (2)$$

Here q_j is the polarization of an individual gas molecule having a velocity $v_j(\theta)$ in the light-wave propagation direction z ; N is the number of particles per unit volume; A_i ($i = 1, 2, p, a$) are the amplitudes of the exciting light pulses ($i = 1, 2$), of the probing wave ($i = p$) and of the anti-Stokes scattering component ($i = a$); $\theta = t - z/c$, T_c is the time of molecular-vibration dephasing as a result of the collisions (the statistical meaning of the time T_c is discussed later on), $k_0 = \omega_0/c$; γ_a

are the nonlinear-coupling coefficients, and ω_0 is the Raman-resonance frequency. The only difference between these equations and the usual equations for condensed media¹⁹ lies in the presence of a Doppler term $ik_0 v_j(\theta) q_j$ in the first equation. In the presence of collisions, $v_j = v_j(\theta)$ is a Gaussian stationary random process.

Writing the solution of (1) in the form of a Duhamel integral (see, e.g., Ref. 30, p. 217) and averaging q_j over the ensemble of the molecules, we obtain

$$Q = \gamma_a \int_0^\infty A(\theta - \theta_1) e^{-\theta_1/T_c} \langle e^{i\varphi_j(\theta, \theta_1)} \rangle d\theta_1, \quad (3)$$

$$\varphi_j(\theta, \theta_1) = k_0 \int_0^{\theta_1} v_j(\theta - t) dt. \quad (4)$$

Since the molecule distribution in velocity v_j is Gaussian, the quantity φ_j defined by Eq. (4) has also a normal distribution.³⁰ Consequently

$$\langle \exp [i\varphi_j(\theta, \theta_1)] \rangle = \exp [-1/2 \langle \varphi_j^2(\theta, \theta_1) \rangle], \quad (5)$$

and the variance of the phase shift can in turn be expressed in terms of the velocity correlation function:

$$\langle \varphi_j^2(\theta, \theta_1) \rangle = k_0^2 \int_0^{\theta_1} \int_0^{\theta_1} B(t_2 - t_3) dt_2 dt_3 = 2k_0^2 \int_0^{\theta_1} (\theta_1 - \tau) B(\tau) d\tau, \quad (6)$$

$$B(\tau) = \langle v_j(t) v_j(t + \tau) \rangle. \quad (7)$$

An important role is played in what follows by the function

$$L(\theta) = k_0^2 \int_0^\theta (\theta - \tau) B(\tau) d\tau. \quad (8)$$

Regardless of the concrete form of $B(\tau)$, this function has the following properties (see Ref. 30, p. 152):

$$L(\theta) = \begin{cases} (k_0 \sigma_v^2 \theta)^2 / 2 & \text{at } \theta \ll \tau_v, \\ k_0^2 D (\theta - \tau_0) & \text{at } \theta \gg \tau_v. \end{cases} \quad (9)$$

Here τ_v is the velocity correlation time, $\sigma_v^2 = B(0) = kT/m$ is the variance of the velocity, k is Boltzmann's constant, T is the absolute temperature, m is the molecule mass,

$$D = \int_0^\infty B(\tau) d\tau = \sigma_v^2 \tau_v, \quad \tau_0 = D^{-1} \int_0^\infty \tau B(\tau) d\tau, \quad (10)$$

where D is the correlation constant of the diffusion coefficient,³⁴ and τ_0 is a time interval of the order of τ_v . The first equation in (10) can be regarded as a definition of the correlation time τ_v . We thus obtain^{31,32}

$$Q(\theta) = \gamma_a \int_0^\infty A(\theta - \theta_1) h(\theta_1) d\theta_1, \quad (11)$$

$$h(\theta) = \exp [-\theta/T_c - L(\theta)]. \quad (12)$$

Let us dwell briefly on the statistical interpretation of the collisional dephasing time T_c . The dephasing due to the collisions of the molecules is described in Eq. (1) by the phenomenological constant T_c . The equation for the polarization q_j of an individual molecule should more rigorously be written in the form^{31,32}

$$\frac{\partial q_j}{\partial \theta} + [\alpha_0 + i\nu_j(\theta)] q_j = \gamma_a A(\theta), \quad (13)$$

where the parameter α_0 characterizes the velocity of the intramolecular relaxation (we neglect hereafter this dephasing mechanism), $\langle v_j(\theta) = v_{jc}(\theta) + v_{jd}(\theta) \rangle$ are the fluctuations of the frequency of the molecular oscillator and are due to collisions and to the Doppler effect, $\langle v_j(t)v_l(t+\tau) \rangle = B_{0l}(\tau)\delta_{jl}$, and δ_{jl} is the Kronecker symbol. We assume that the fluctuations $v_{jc}(\theta)$ and $v_{jd}(\theta) = -k_0 v_j(\theta)$ are statistically independent Gaussian stationary random processes, and furthermore that the following condition is satisfied:

$$\sigma_c^2 \tau_c^2 \ll 1, \quad (14)$$

where σ_c^2 is the variance and τ_c is the correlation time of the fluctuations $v_{jc}(\theta)$. The expression for the total polarization Q of the medium can then be represented in the form (3), where

$$T_c^{-1} = \pi G_c(0) = \sigma_c^2 \tau_c, \quad (15)$$

$G_c(\omega)$ is the spectrum of the frequency fluctuations $v_{jc}(\theta)$ due to the collisions. The collisional dephasing time T_c , introduced earlier phenomenologically, is thus expressed in terms of the spectrum of the fluctuations $v_{jc}(0)$ at zero frequency.¹¹

If it is assumed that $\tau_c \approx \tau_v$, the condition (14) can be rewritten in the form $\tau_v/T_c \ll 1$. Since $\tau_v/T_c = 0.019$ for hydrogen (see below), the condition (14) can be assumed satisfied.

We have carried out concrete calculations based on Eqs. (11) and (12) for two models of the velocity correlation function $B(\tau) = \sigma_v^2 R(\tau)$:

$$R_1 = e^{-|y|}, \quad L_1 = \beta(y-1+e^{-y}) \quad (16)$$

and

$$R_2 = (1+y^2)^{-1/2}, \quad L_2 = \beta[(1+y^2)^{1/2}-1]. \quad (17)$$

The functions L_1 and L_2 were calculated here from Eq. (8) and the notation $y = \tau/\tau_v$, $\beta = (k_0 \sigma_v \tau_v)^2$ was used. In both cases

$$\int_0^\infty R(y) dy = 1.$$

Plots of the correlation coefficients $R(y)$ and of the functions $L(y)$ are shown in Fig. 5. As can be seen from the figure, in the region $y \ll 1$ the functions L_1 and L_2 are equal with a value $L(y) = \beta y^2/2$, in accord with Eq. (9). At larger values of the argument ($y \gg 1$) the functions L_1 and L_2 likewise tend to a common limit $L(y) = \beta(y-1)$. The difference between L_1 and L_2 reaches a maximum in the region $1 < y < 5$ and amounts to approximately 10%. Nonetheless, an analysis of the experimental data on time-domain CARS of hydrogen (see below and Fig. 3) makes the exponential model (16) preferable. A substantial role is played here by the large range of variation of the CARS signal (5 decades).

The derived equations (11), (12), (8), (16), and (17) together with Eq. (2) for the amplitudes A_a of the anti-Stokes component permit us to describe both the frequency and the pulsed variants of CARS of an inhomogeneously broadened

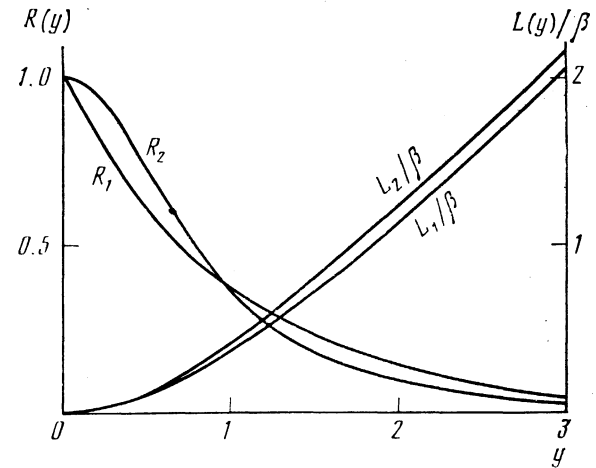


FIG. 5. Models of correlation function of thermal velocities $R(y)$ and the functions $L(y)$ corresponding to them.

transition with arbitrary pumping: continuous, steplike, pulsed, noise, etc. We proceed now to calculate the time-domain CARS signal.

Since the duration of the light pulses used in the experiments ($\tau_{\text{pul}} = 40$ psec) is much shorter than the dephasing time of the molecular vibrations ($\tau_{\text{ph}} \approx 1$ nsec), the exciting and probing pulses can be regarded as δ -pulses: $A(\theta) \propto (W_1 W_2)^{1/2} \delta(\theta)$, $I_p(\theta) \propto W_p \delta(\theta - \tau)$, where W_1 , W_2 and W_p are the energies of the exciting and probing pulses, and τ is the delay of the probing pulse relative to the exciting ones. By virtue of (11) we then obtain at $\theta > 0$

$$Q(\theta) \propto (W_1 W_2)^{1/2} h(\theta). \quad (18)$$

From (2) we have $A_a = \gamma_a A_p Q(\theta) z$. We have then for the radiation intensity at the anti-Stokes frequency $I_a \propto I_p |Q|^2 z^2$. The energy of the anti-Stokes pulse is

$$W_a(\tau) \propto \int_{-\infty}^{\infty} I_a(\theta) d\theta \propto W_p |Q(\tau)|^2 z^2, \quad (19)$$

or, taking (18) into account

$$W_a(\tau) = W_a(0) h^2(\tau), \quad (20)$$

where $W_a(0) \propto W_1 W_2 W_p z^2$ is the energy of the pulsed response at zero delay and $h(\tau)$ is a real function defined by (12). We obtain thus

$$\ln [W_a(\tau)/W_a(0)] = \ln h^2(\tau) = -2[\tau/T_c + L(\tau)], \quad (21)$$

where the function $L(\tau)$ is defined by (16) or (17).

COMPARISON OF THE THEORETICAL AND EXPERIMENTAL DATA

The derived equations (21), (16), and (17) permit a quantitative interpretation of the experimental data on time-domain CARS of hydrogen, shown in Figs. 3 and 4. The time of collisional dephasing and the time τ_v of the correlation of the thermal velocities of the hydrogen molecules will be determined by inspection by starting from the experimental data. Both quantities are proportional to the mean free path time of the molecules; therefore

$$T_c = a\rho^{-1}, \quad \tau_v = b\rho^{-1}, \quad (22)$$

where a and b are independent of pressure and are parameters of the material, and ρ is the gas density in amagats. Our estimates for hydrogen yield

$$a = 6.9 \pm 0.5 \text{ nsec}, \quad b = 0.13 \pm 0.02 \text{ nsec}. \quad (23)$$

At these values, the theoretical plots based on Eqs. (21), (16), (17), and (22) lie closest to the experimental points (see Figs. 3 and 4).

These estimates of the constants a and b agree well with the available published data. Thus, the spontaneous Raman-scattering pressure coefficient of spontaneous Raman scattering measured in Ref. 1 is $\Delta\nu/\rho = 0.0015 \pm 0.0001 \text{ cm}^{-1}/\text{amagat}$. In the high-pressure limit, $\Delta\nu = (\pi c T_c)^{-1}$. Hence $a = 7.1 \pm 0.5 \text{ nsec}$. The velocity correlation time is connected with the gas-diffusion coefficient $D = \sigma_v^2 \tau_v = D_0/\rho$ [see (10)]. From the data of Refs. 1 and 6, the constant D_0 for hydrogen lies in the range $D_0 = 1.40 \pm 0.05 \text{ cm}^2 \cdot \text{amagat}/\text{sec}$. Consequently $b = 0.115 \pm 0.005 \text{ nsec}$.

Analysis of the experimental data, carried out for two different models (16) and (17) of the velocity correlation function, leads to the following conclusions (see Fig. 3). At pressures higher than 1 atm and lower than 5 Torr both models yield the same result. In the pressure range from 50 to 400 Torr the data of the two models differ, with model (16) describing the experimental data more accurately (error less than 10%) than those of model (17) (error 15–20%).

Using the general expression (8) for the function $L(\theta)$, it is easy to show that

$$\frac{d^2}{d\tau^2} \ln \frac{W_a(0)}{W_a(\tau)} = 2 \frac{d^2 L(\tau)}{d\tau^2} = 2k_0^2 B(\tau). \quad (24)$$

It follows hence that the form of the velocity correlation function can in principle be determined.^{31,32} To calculate $B(\tau)$ from this equation, however, $W_a(\tau)$ must be measured with sufficiently high accuracy, since the relative signal fluctuations increase steeply after differentiating twice.

From (9), (12), (20), and (22) it follows that the contour of the response pulse is independent of the form of $B(\tau)$ in the limits of low (Doppler limit) and high (Lorentz limit) pressures. In the low-pressure limit

$$W_a(\tau)/W_a(0) = \exp[-(k_0 \sigma_v \tau)^2], \quad (25)$$

i.e., the energy of the anti-Stokes radiation decreases in Gaussian fashion with increasing delay. In the high-pressure limit the pulsed response attenuates exponentially:

$$\ln [W_a(\tau)/W_a(0)] = -2[1/T_c + (k_0 \sigma_v)^2 \tau_v] \tau. \quad (26)$$

Since both T_c and τ_v decrease with increasing pressure, at a certain pressure the slope of the straight line $\ln [W_a(\tau)/W_a(0)]$ is a minimum (Dicke narrowing). By introducing the ratio $\tau_v/T_c = \alpha$, which is independent of pressure and is a parameter of the investigated molecules, it is easy to determine the position of the minimum slope: $\rho_0 = a k_0 \sigma_v \sqrt{\alpha}$. For hydrogen we have $a = 6.9 \text{ nsec}$, $k_0 = 2.61 \times 10^4 \text{ cm}^{-1}$, $\sigma_v = 1.1 \times 10^5 \text{ cm/sec}$, $\alpha = 0.019$, $T = 293$, and an estimate using the derived formula shows

that the minimum linewidth is reached at a pressure 2.9 atm, which agrees with the spectral-measurement data.^{1,4,6}

MOLECULAR-VIBRATION DEPHASING TIME

We define the molecular-vibration dephasing time τ_{ph} as the time during which the energy of the pulsed response, measured in the time-domain CARS, decreases by a factor $\exp(2m)$ (Ref. 32):

$$W_a(\tau_{ph})/W_a(0) = \exp(-2m). \quad (27)$$

Here m is some positive number. The dephasing time characterizes the relaxation rate of the coherent response of the medium and is useful because, on the one hand, it is directly measurable and on the other, it is easy to calculate. In fact, it follows from (21) that τ_{ph} is the solution of the equation

$$\tau_{ph}/T_c + L(\tau_{ph}) = m, \quad (28)$$

whence we obtain for the exponential model of $B(\tau)$ (16)

$$\alpha y + \beta(y-1+e^{-y}) = m. \quad (29)$$

Here $\alpha = \tau_v/T_c = b/a$, $\beta = (k_0 \sigma_v \tau_v)^2$, and $y = \tau_{ph}/\tau_v$. We introduce the variable $u = \rho/\rho_0$, where ρ_0 is the gas density at which the Dicke narrowing has a maximum. Then $\beta = \alpha/u^2$, $\tau_{ph} = y\sqrt{\alpha}/uk_0\sigma_v$, and consequently the dependence of the dephasing time on the normalized gas density u is a function of only one parameter of the investigated molecules, α . Figure 6 shows the dependence of the dephasing time on the hydrogen density, obtained by solving Eq. (29) with $\alpha = 0.019$. The figure shows also the experimental points of this dependence. It can be seen that the observed and theoretical values agree.

Using the properties of the function $L(\theta)$ [see (9)], we represent the solution of (28) at large values of the parameter m in the form

$$\tau_{ph} = \frac{m}{1/T_c + (k_0 \sigma_v)^2 \tau_v} = \frac{m}{k_0 \sigma_v \sqrt{\alpha}} \left(\frac{u}{1+u^2} \right). \quad (30)$$

It follows therefore that at large values of m the dependence of τ_{ph} on the gas density always has a maximum (at $u = 1$). At the same time, the narrowing of the spectral lines as a

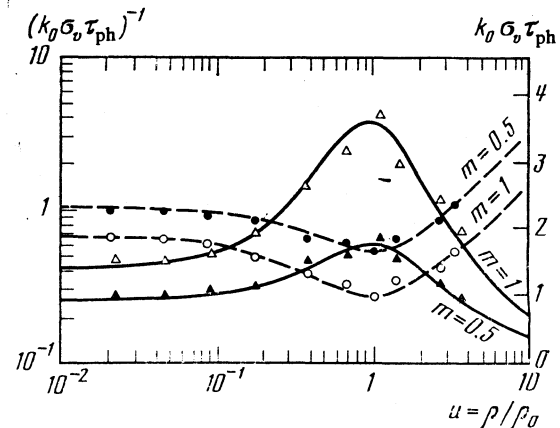


FIG. 6. Dephasing time of molecular vibrations in hydrogen vs gas density. Continuous curves—dephasing time, dashed—reciprocal dephasing time, the analog of the linewidth.

result of the Dicke effect can be observed not always, but only when the parameter α is small enough: $\alpha < 0.35$ (Ref. 32).

SPECTROSCOPIC INFORMATION IN STEADY-STATE AND TIME-DOMAIN CARS

In steady-state CARS one measures the radiation intensity at the anti-Stokes frequency as a function of the frequency detuning $\omega = \omega_1 - \omega_2 - \omega_0$ relative to the line center. Such measurements yield information on the frequency dispersion of the modulus of $\chi^{(3)}$ of the cubic susceptibility of the material.¹⁹ We shall show here that in the case of a solitary line and the Doppler mechanism of the inhomogeneous dephasing of the molecular vibrations the time-domain CARS method makes it possible, in principle, to determine not only the modulus but also the phase of $\chi^{(3)}$.^{31,32}

The amplitude of the polarization at the anti-Stokes frequency can be written in the form¹⁹

$$\mathcal{P}_{nl}(\omega_a) = \frac{1}{2} N \alpha' A_p Q = 6 \chi^{(3)}(\omega_a, \omega) A_p A_1 A_2^*, \quad (31)$$

where α' is the derivative of the electronic polarizability of the molecule with respect to coordinate. From this and from (11) we obtain at $A(\theta) = A_1 A_2^* = A_0 \exp i \omega \theta$, $A_0 = \text{const}$

$$\chi^{(3)}(\omega) = \frac{1}{12} N \alpha' \gamma_q \chi(\omega), \quad (32)$$

where

$$\chi(\omega) = \int_0^{\infty} h(\theta) e^{-i\omega\theta} d\theta \quad (33)$$

is the polarization susceptibility of the medium. From this we have by virtue of (20)

$$\chi^{(3)}(\omega) = \frac{1}{12} N \alpha' \gamma_q \int_0^{\infty} \left[\frac{W_a(\theta)}{W_a(0)} \right]^{1/2} e^{-i\omega\theta} d\theta, \quad (34)$$

where $W_a(\tau)$ is the energy of the pulsed response. Since $W_a(\tau < 0) = 0$, the lower limit in the integral of (34) can be replaced by $-\infty$. The pulsed-response function measured in the time-domain CARS is thus connected by a Fourier transformation with the complex nonlinear susceptibility. We note, however, that the indicated connection between $W_a(\tau)$ and $\chi^{(3)}(\omega)$ exists only in the case of a symmetrical distribution $w(\varphi_j)$ of the random phase shift φ_j due to the inhomogeneous dephasing. If, however, the distribution $w(\varphi_j)$ is not symmetric (e.g., in rotational dephasing), the Green's function $h(\theta) = \exp(-\theta/T_c) \langle \exp(i\varphi_j) \rangle$ becomes complex and measurement of the pulsed response $W_a(\tau) \propto |h(\tau)|^2$ does not make it possible to determine $h(\tau)$ and to calculate $\chi^{(3)}(\omega)$ from Eqs. (32) and (33).

The signal intensity in steady-state CARS is

$$I_a(\omega) \propto |\chi^{(3)}(\omega)|^2. \quad (35)$$

For $\chi^{(3)}(\omega)$ defined by Eqs. (32), (33), (12), and (16), an analogous expression was obtained earlier in Ref. 3. Let us dwell briefly on the case of extremely low energies (the Doppler limit). In this case

$$I_a(\omega) \propto \left| \int_0^{\infty} \exp[-(k_0 \sigma_v)^2 / 2] e^{-i\omega\theta} d\theta \right|^2. \quad (36)$$

The integral in (36) is expressed in terms of the error function of complex argument: $I_a(\omega) \propto |w(s)|^2$, where $s = \omega / (\sqrt{2} k_0 \sigma_v)$,

$$w(s) = e^{-s^2} \left[1 + \frac{2i}{\sqrt{\pi}} \int_0^s e^{x^2} dx \right]. \quad (37)$$

This result was obtained in Refs. 40 and 41, devoted to a calculation of the spectrum in steady-state CARS in the Doppler limit. As shown in these papers, the line $|w(s)|^2$ is Gaussian in shape at the center and Lorentzian on the wings. Thus, first, the rather pulsed response recorded in the Doppler limit in time-domain CARS corresponds to a rather complicated spectrum in the steady-state CARS. Second, the information obtained by measuring the pulsed response and by taking its Fourier transform is more complete, since it permits calculation of the modulus of the susceptibility $\chi^{(3)}(\omega)$ as well as its phase.

In conclusion, we formulate our main results.

1. Experimental data were obtained on time-domain CARS of hydrogen in a wide range of pressures, from the Doppler limit to the homogeneous broadening limit, including the Dicke narrowing region.

2. The shape of the pulsed response in time-domain CARS was calculated for arbitrary gas pressure.

3. The experimental data and calculations were used to estimate the time of collisional dephasing and the correlation time of the thermal velocities in hydrogen.

4. It was shown that the time-domain CARS method yields the real and imaginary components of the nonlinear susceptibility $\chi^{(3)}(\omega)$ of the medium, in contrast to the frequency-domain variant of CARS, in which $|\chi^{(3)}(\omega)|^2$ is measured.

5. The time-domain CARS signal was calculated for two models of the correlation coefficient of the thermal velocities of the molecules: $R_1 = \exp(-|y|)$ and $R_2 = (1 + y^2)^{-3/2}$, where $y = \tau/\tau_v$ and τ_v is the correlation time. If we established that the model $R_1(\tau)$ describes more accurately the experimental data on hydrogen (error less than 10%) than the model $R_2(\tau)$ (error 15–20%).

The authors are deeply grateful to S. A. Akhmanov for constant interest in the work and for helpful discussions.

¹⁹A similar result was obtained in the theory of dephasing of molecular vibrations in liquids (see Refs. 35–39, as well as Ref. 19, Chap. V, §5).

¹J. R. Murray and A. Javan, *J. Mol. Spectrosc.* **42**, 1 (1972).

²J. M. Cherlow and S. S. P. Porto in: *Laser Spectroscopy of Atoms and Molecules*, Springer, 1976. Russ. transl. Mir, 1979, p. 293.

³F. de Martini, F. Simoni, and E. Santamato, *Opt. Commun.* **9**, 176 (1973).

⁴M. A. Henesian, L. Kulevskii, R. L. Byer, and R. L. Herbst, *Opt. Commun.* **18**, 225 (1976).

⁵B. B. Krynetsky, L. A. Kulevsky, V. A. Mishin *et al.*, *ibid.* **21**, 225 (1977).

⁶A. Owyong, *Opt. Lett.* **2**, 9 (1978).

⁷E. D. Hinckley, C. V. Hill, and F. A. Blum, *Ref. 2*, Russ. p. 155.

⁸R. Brewer, in: *Nonlinear Spectroscopy*, N. Bloembergen, ed., Am. Elsevier, 1977. Russ. transl. Mir, 1979, p. 119.

⁹R. L. Shoemaker, in: *Laser and Coherence Spectroscopy*, J. I. Steinfeld, ed. Plenum Press, Chap. 3.

¹⁰T. Schmalz and W. H. Flygare, *ibid.* Chap. 2.

¹¹B. Comaskey, R. E. Scotti, and R. L. Shoemaker, *Opt. Lett.* **6**, 45 (1981).

- ¹²A. Laubereau and W. Kaier, *Rev. Mod. Phys.* **50**, 607 (1978).
- ¹²W. Kaier and A. Laubereau, *Ref.* **8**, Russ. p. 528.
- ¹⁴M. Matsuoka, H. Nakatsuka, and J. Okada, *Phys. Rev.* **A12**, 1062 (1975).
- ¹⁵B. I. Green, R. B. Weisman, and R. M. Hochstrasser, *Chem. Phys. Lett.* **59**, 5 (1978).
- ¹⁶M. S. Dzhidzhoev, S. A. Magnitskii, A. P. Tarasevich, V. G. Tunkin, and A. I. Kholodnykh, Abstracts, 10th All-Union Conf. on Coherent and Nonlinear Optics, M. 1980, Part 2, p. 170.
- ¹⁷M. S. Dzhidzhoev, S. A. Magnitskii, S. M. Saltiel, *et al.*, *Kvant. Elektron. (Moscow)* **8**, 1136 (1981) [*Sov. J. Quantum Electron.* **11**, 681 (1981)].
- ¹⁸S. A. Magnitskii and V. G. Tunkin, *Kvant. Elektron. (Moscow)* **8**, 2008 (1981) [*Sov. J. Quantum Electron.* **11**, 1218 (1981)].
- ¹⁹S. A. Akhmanov and N. I. Koroteev, *Metody nelineinoi optiki v spektroskopii rasseyaniya sveta (Nonlinear Optics Methods in Light-Scattering Spectroscopy)*, Nauka, 1981.
- ²⁰J. P. Wittke and R. H. Dicke, *Phys. Rev.* **103**, 620 (1956).
- ²¹L. Galatry, *Phys. Rev.* **122**, 1218 (1961).
- ²²S. G. Rautian and N. I. Sobel'man, *Usp. Fiz. Nauk* **90**, 209 (1966) [*Sov. Phys. Usp.* **9**, 701 (1967)].
- ²³V. S. Letokhov and V. P. Chebotaev, *Nonlinear Laser Spectroscopy*, Springer, 1977.
- ²⁴V. S. Averbakh, A. A. Betin, V. A. Gaponov, *et al.*, *Izv. Vyssh. Ucheb. Zaved. Radiofizika* **21**, 1077 (1978).
- ²⁵L. A. Vainshtein, I. I. Sobel'man, and E. A. Yukov, *Vozbuzhdenie atomov i ushirenie spektralnykh linii (Atom Excitation and Spectral-Line Broadening)*, Nauka, 1979.
- ²⁶S. G. Rautian, G. I. Smirnov, and A. M. Shalagin, *Nelineinye rezonansy v spektrakh atomov i molekul (Nonlinear Resonances in the Spectra of Atoms and Molecules)*, Nauka, Novosibirsk, 1979.
- ²⁷V. A. Alekseev and A. V. Malyugin, *Zh. Eksp. Teor. Fiz.* **80**, 897 (1981) [*Sov. Phys. JETP* **53**, 447 (1981)].
- ²⁸V. P. Kachanov and V. P. Lopasov, in: *Spektral'nye proyavleniya mezhmolekulyarnykh vzaimodeistvii v gazakh (Spectral Manifestations of Intermolecular Interactions in Gases)*, Nauka, Novosibirsk, 1982, p. 142.
- ²⁹S. Chandrasekhar, *Rev. Mod. Phys.* **15**, 1 (1943).
- ³⁰S. A. Akhmanov, Yu. A. D'yakov, and A. S. Chirkin, *Vvedenie v statisticheskuyu radiofiziku i optiku (Introduction to Statistical Radiophysics and Optics)*, Nauka, 1981.
- ³¹Yu. E. D'yakov, *Éffekty defazirovki i impul'snoi korrelyatsionnoi i chastotnoi spektroskopii (Dephasing Effects in Pulsed Correlation and Frequency-Domain Spectroscopy)*, Preprint, Phys. Inst. Moscow State Univ., 1983.
- ³²Yu. E. D'yakov, *Pis'ma Zh. Eksp. Teor. Fiz.* **37**, 14 (1983) [*JETP Lett.* **37**, 15 (1983)].
- ³³Yu. D'yakov and S. Yu. Nikitin, Abstracts, 11th All-Union Conf. on Coherent and Nonlinear Optics, Erevan, 1982, part I, p. 243.
- ³⁴P. T. Landsberg, *Problems in Thermodynamics and Statistical Physics*, Academic, 1971. Russ. transl. Mir, 1974, p. 430.
- ³⁵S. F. Fischer and A. Laubereau, *Chem. Phys. Lett.* **35**, 6 (1975).
- ³⁶R. M. Lynden-Bell, *Mol. Phys.* **33**, 907 (1977).
- ³⁷D. W. Oxtoby, D. Levesque, and J. Weis, *J. Chem. Phys.* **68**, 5528 (1978).
- ³⁸D. J. Diestler, *Chem. Phys. Lett.* **39**, 39 (1976).
- ³⁹C. H. Wang, *Mol. Phys.* **33**, 207 (1977).
- ⁴⁰M. A. Hennesian and R. L. Byer, *J. Opt. Soc. Am.* **68**, 648 (1978).
- ⁴¹S. A. Druet and J. P. Taran, *J. de Phys.* **40**, 819 (1979).

Translated by J. G. Adashko